Date: 12/29/17

EIC Detector R&D Progress Report

Project ID: eRD1
Project Name: EIC Calorimeter Development
Period Reported: from 7/1/17 to 12/31/17
Project Leaders: H.Huang and C.Woody
Contact Persons: O.Tsai, T.Horn, C.Woody, S.Kuleshov, E.Kistenev

Collaborators

S.Boose, J.Haggerty, J.Huang, E.Kistenev, E.Mannel, C.Pinkenberg, M. Purschke, S. Stoll and C. Woody
(PHENIX Group, BNL Physics Department)

E. Aschenauer, S. Fazio, A. Kiselev
(Spin and EIC Group, BNL Physics Department)

Y. Fisyak
(STAR Group, Physics Department)
Brookhaven National Laboratory

L. Zhang and R-Y. Zhu
California Institute of Technology

S. Ali, V. Berdnikov, T. Horn, I. Pegg, R. Trotta, A. Vargas
The Catholic University of America and
Thomas Jefferson National Accelerator Facility

W. Jacobs, G. Visser and S. Wissink
Indiana University

A. Hernandez, Y. Kim, A. Sickles
University of Illinois at Urbana Champaign

G. Hull, M. Josselin, C. Munoz-Camacho, H. San, R. Wang
IPN Orsay, France

L. Dunkelberger, H.Z. Huang, K. Landry, M. Sergeeva, S. Trentalange, O. Tsai
University of California at Los Angeles

S.Kuleshov, Eliás Rozas, Pablo Ulloa, Lautaro León
Federico Santa María Technical University (UTFSM), Valparaiso, Chile

A.Denisov, A.Durum,
Institute for High Energy Physics, Protvino, Russia
A.Brandin, MEPHI, Russia

H. Mkrtychyan
Yerevan Physics Institute

Abstract & Summary

This report summarizes the activities of the eRD1 Calorimeter Consortium during the period from July 1, 2017 – December 31, 2017. These activites are divided into four Sub-Projects: Tungsten Calorimeter R&D at UCLA, Tungsten Calorimeter R&D at BNL (sPHENIX), R&D on Crystal Calorimeters, and R&D on a High Resolution Tungsten Shashlik Calorimeter for EIC. The last project is a new effort that aims to develop a new calorimeter technology for EIC and brings new international participation to the eRD1 Consortium.

The effort on tungsten calorimeter R&D is based on the tungsten powder scintillating fiber (W/SciFi) design originally developed at UCLA and is focused on the development of an electromagnetic calorimeter for the central and/or mid rapidity region at EIC. The effort at UCLA was mainly on studing the readout sensors (SiPMs an APDs) and how they behave in the radiation environment at RHIC. Samples of both types of sensors were placed in the STAR Experimental Hall for Run 17 and changes were measured in sensor response, breakdown voltage and noise after exposure to the particle flux in the hall during Run 17. Significant changes were measured and differences were seen between different devices at the same location. The effort at BNL was mainly focused on the sPHENIX EMCAL and on completing the design of a new 2D projective prototype. This prototype will include improved absorber blocks, new light guides and new readout electronics and will be tested in the test beam at Fermilab in early 2018. New absorber blocks were produced at UIUC which should have better light collection and uniformity than the ones used in the previous prototype, and new injection molded light guides were obtained that are of excellent optical quality and can be produced at low cost. The sPHENIX effort is being funded entirely from sPHENIX funds, but its progress is reported here since it is highly connected with the development of a W/SciFi calorimeter for EIC.

The R&D effort on crystal calorimetry continues to focus on the development of a lead tungstate (PWO) calorimeter for the electron endcap. As stated in our previous report, a critical aspect for crystal quality, and thus resolution performance of the EIC inner endcap calorimeter, is the combination of high light output, uniform light collection and good radiation hardness, all of which depend on the crystal manufacturing process. Our previous studies have shown that there is significant crystal-to-crystal variation for crystals manufactured by SICCAS. Evaluation of the variation in the chemical composition and optical properties from crystal to crystal is one of the main goals of this R&D project, and, by working together with the vendors, we hope to determine the origin of this variation. Our previous studies also showed that systematic effects such as non-uniformities in light collection, which are in part properties of the crystal itself, have a large impact on the constant term in the calorimeter energy resolution. Therefore, another main goal over the next year is to explore ways to reduce the contribution of these effects to the constant term. The availability of a sufficient number of high quality crystals to construct a small prototype calorimeter to study these effects is also critical. This prototype would allow for studies of the crystals in the test beam in order to measure the actual energy and position resolution, including the constant term, and to test different readout systems. However, we have so far not been able to pursue the construction of this prototype calorimeter due to lack of funding.

The effort on the shashlik calorimeter is focused on the development of a high density, fully projective shashlik electromagnetic calorimeter with improved energy, position and timing resolution for EIC. This calorimeter would address the specific needs for EIC in terms of studying hard scattering processes in the central region by measuring jets and providing particle ID for particles produced in SIDIS and DVCS events down to low transverse momenta. The calorimeter is based on a shashlik deign with a SiPM readout and will utilize an alloy of tungsten and copper (80W20Cu) that allows easy machining and drilling of the absorber plates. It will also utilize injection molded scintillating tiles that are readily produced at IHEP and/or at UNIPLAST in Russia. This project received no funding from EIC in FY18, but technical progress has been proceeding using other external funds and is reported on here.

Sub Project 1: Progress on Tungsten Powder Calorimeter R&D at UCLA

Project Leaders: H.Z. Huang and O. Tsai

What was planned for this period?

We planned to characterise all exposed SiPMs during Run 17 at RHIC in the lab. In total, we tested about 160 SiPMs exposed in the Run 17 at 125 cm and 35 cm away from the beam line as well as many unexposed SiPMs. We investigated the following questions:

- Is the degradation in response the same for sensors located at the same positions?
- Do we see a change in bias voltage Vbd and is the change the same for different sensors?
- Does the degradation in response depend on the shape of the light pulse?
- Noise as a function of ΔV and gate width
- Effect of increased after pulses, trap lifetime and high hit rate
- Excess noise factor, by direct comparison of the response of the HCAL and EMCal to cosmic muons (exposed/unexposed sensors, both SiPMs and APDs).

What was achieved?

We investigated most of the questions above. Our conclusions can be summarized briefly as follows:

- SiPMs will work reasonably well as readout sensors for sampling calorimeters at EIC with the proposed choice of tungsten/fiber calorimeter technology
- Performance of SiPMs is expected to degrade under EIC running conditions
- Potentially, every SiPM is 'unique' and will degrade/recover differently depending upon exposure
- A good monitoring system for any calorimeters utilizing SiPMs is necessary
- Future calculations of radiation damage may need to be refined
- Future developments of the readout for sampling calorimeters at EIC based on APDs probably will not be an urgent task.

The large sample of SiPMs available for these studies were initially intended for studies of anomalous signals caused by primary ionization in the sensors reported six months ago. The STAR FEMC was equipped with 32 readout boards. Each board had 4 pre-selected SiPMs (operation voltage within 10 mV based on HPK data). All of these boards were located in an volume of 10 x 10 x 2.5 cm^3 at a distance ~135 cm from the beam line, i.e. in close proximity to each other, and are assumed in the same exposure conditions. Un-mounted SiPMs were located within a volume at a distance ~43 cm from the beam line.

To measure the degradation in their response we made a direct comparison of the responses of exposed boards (or single SiPMs) to unexposed boards (SiPMs) to the same incident light under the same conditions using the same readout chain and protocol. The block diagram of the experimental setup is shown in Fig 1.1

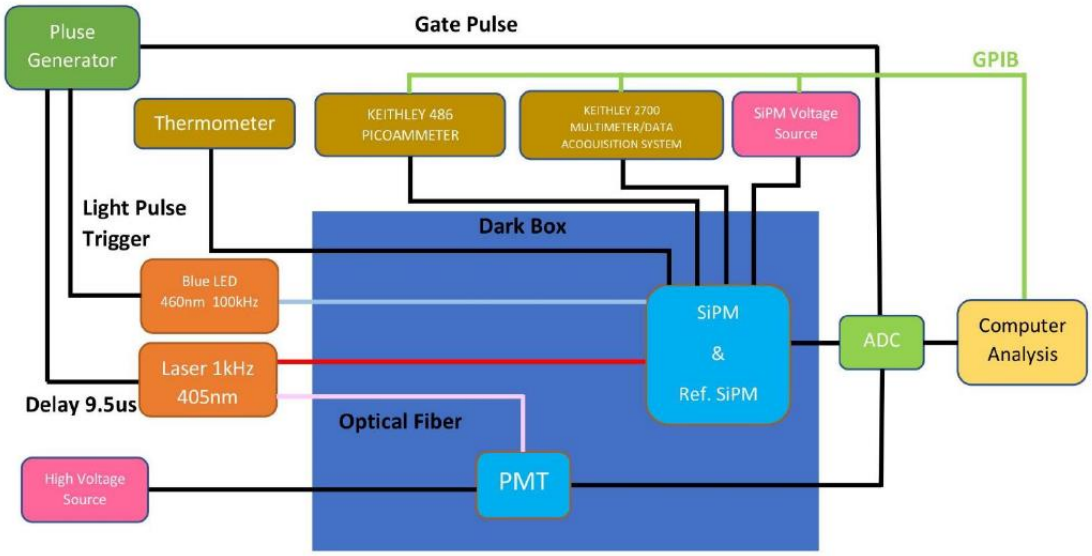

Figure 1.1 Block diagram of setup.

With our setup and test procedures we were able to keep systematics errors within 0.5%. We found that un-exposed SiPMs from two different production batches (serial # 5xxx and 13xxx) had a 2% difference in their response for the nominal Vop specified by HPK, for which we made additional corrections (labelled in plots as batch 1, batch 2 or batch corrections).

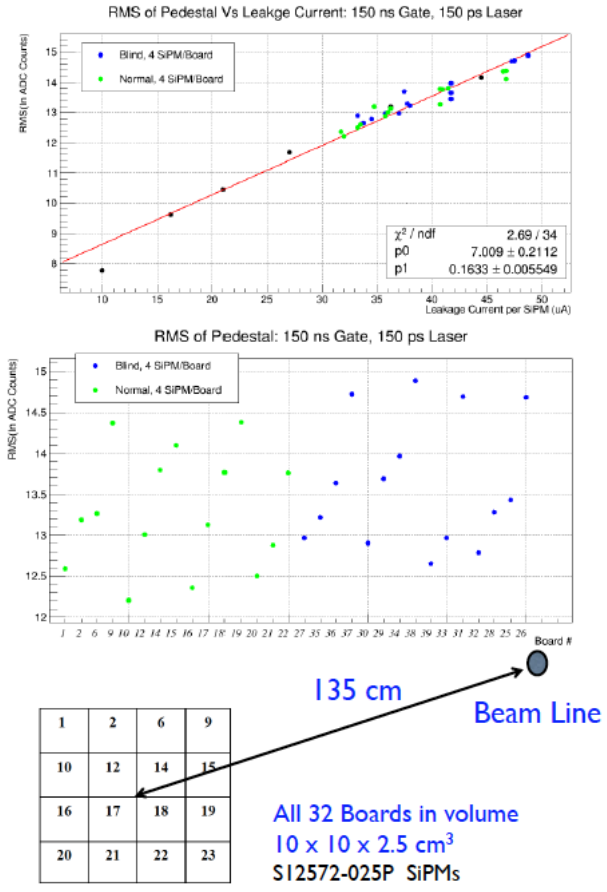

Figure 1.2 Noise after exposure vs leakage current and board position.

Figure 1.2 shows the dependence of the noise on exposed boards vs leakage current, noise vs board ID and a sketch of the setup at the STAR IP. It was somewhat unexpected that the leakage current (exposure) varied by ~30%, being systematically higher for boards which were located closer to the beam pipe. The naïve expectation was that all of these boards would have approximately same exposure at this distance from the beam pipe given the proximity of their locations. The same effects were observed for sensors located at 43 and 46 cm from the beam line, where in this case, the difference in the leakage current was 30%. Probably, some relatively small calorimeter blocks used in Run17 worked as a shield for particles originating from the beam pipe, DX magnet and vacuum pump, which are major sources of neutrons (and other particles) at this location. Potentially, one

would need to know the spectra of particles in this region and convolute these with the damage functions in order to explain the observed dependence of the leakage current on the location of the sensors. Beam background effects cannot be excluded as well.

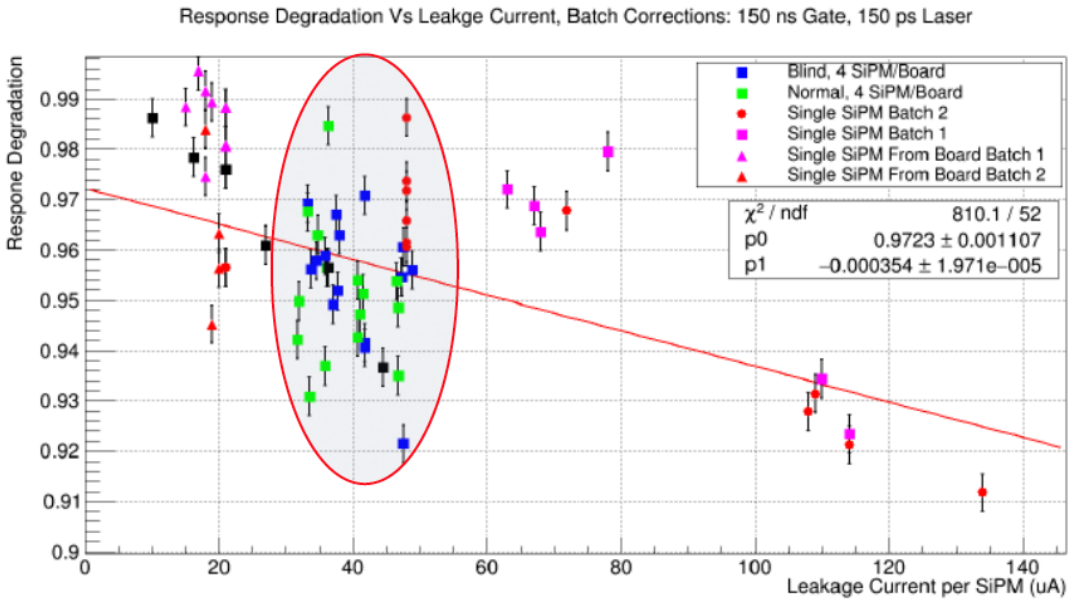

Figure 1.3. Response degradation vs leakage current.

Figure 1.3 shows the degradation in the response of exposed sensors compared to un-exposed sensors vs leakage current. The circle indicates data from the 32 boards described above, where the response from one board is a sum of the responses of four SiPMs. The degradation in the responses is correlated weakly with leakage current (exposure), which confirms our preliminary observations reported at the July meeting. In the particular case of the FEMC readout, one would need to rely on a monitoring system to correct for these changes in response. Making corrections relying just on leakage current (which is relatively easy to monitor) will lead to an additional contribution of ~ 1.6% to the constant term in energy resolution.

The next question we investigated is what happened to individual SiPMs, i.e. whether all four SiPMs from a single FEE board degraded the same way or differently. This is important to know, because in the case of a light collection scheme when light is only partially mixed (as in the case of the FEMC), differential degradation of SiPMs will lead to additional non-uniformities in response. In such a case, even a good monitoring system will be of limited use because the signals from four SiPMs are passively summed at the FEE. Figure 1.4 shows distribution of responses for individual SiPMs from the same FEE board when each of the SiPMs is illuminated separately by the same light source (an optical fiber illuminating the SiPM face). The width of the distribution is consistent with the initial

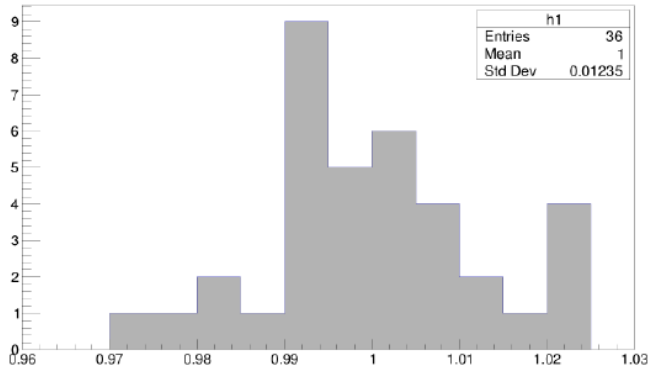

Figure 1.4 Differential degradation of SiPMs.

spread before exposure in the responses according to the HPK data. Note that for each FEE board, the SiPMs have already been preselected to have the same operational bias within 10 mV for convenience of operation. Seemingly, SiPMs which have similar responses at the same bias voltage degraded the same way. Thus, such pre-selection of SiPMs, as in the case of the readout schemes of the FEMC or sPHENIX EMCAL, will reduce the risk of increasing the constant term due to partially mixed light and differential degradation in the responses of the SiPMs with exposure.

We looked at possible reasons of the degradation with exposure. There were reports from CMS that the breakdown voltage changes with the exposure. We investigated several methods of extracting breakdown voltage on exposed senosors from the IV curves and settled on the method of the logarithmic derivative described in the paper by A.N. Otte et. al. https://arxive.org/abs/1606.05186. We checked this method on un-exposed sensors and compared the results with a standard method of extracting the breakdown voltage by measuring the distance between the single photoelectrons peaks vs bias voltage and got consistent results. To assure we have enough sensitivity (1% in response change requires ~ 10 mV change in bias overvoltage), we also mesured the change in Vbd with temperature as shown in Figure 1.5.

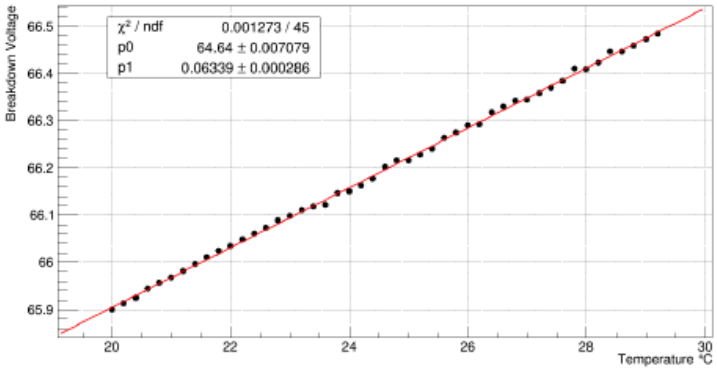

Figure 1.5. Vbd vs temperature.

Prior to these investigations, we had assumed that for a given gain (response), for example, as it is provided by HPK, all sensors should operate at the same overvoltage. That turned out to be incorrect. Since prior to exposure in Run17 we did not characterise the SiPMs Vbd, we had to rely on a sampled average (Vop –Vbd) for the exposed and un-exposed sensors. Figure 1.6 shows this comparison.

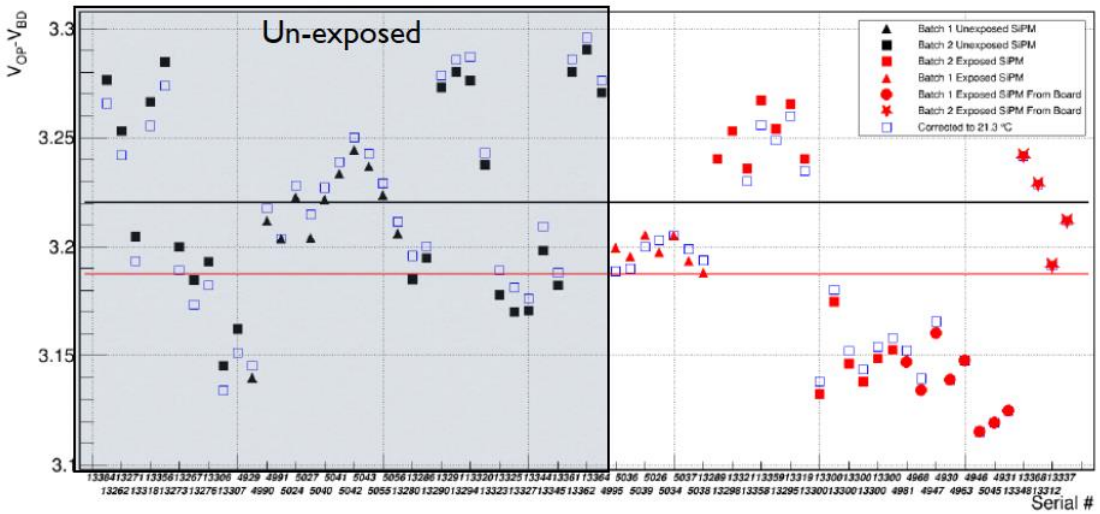

Figure 1.6. Vop-Vbd for exposed and un-exposed sensors.

On average, we see a downward shift in overvoltage of about 30 mV, which qualitatively agreed with the response degradation shown in Figure 1.3. There is no clear correlation between changes in Vop-Vbd and leakage current as shown in Figure 1.7. In Run 18 we plan to expose all characterised sensors again and then measure the change in Vop-Vbd once more, and this will hopefully settle this question.

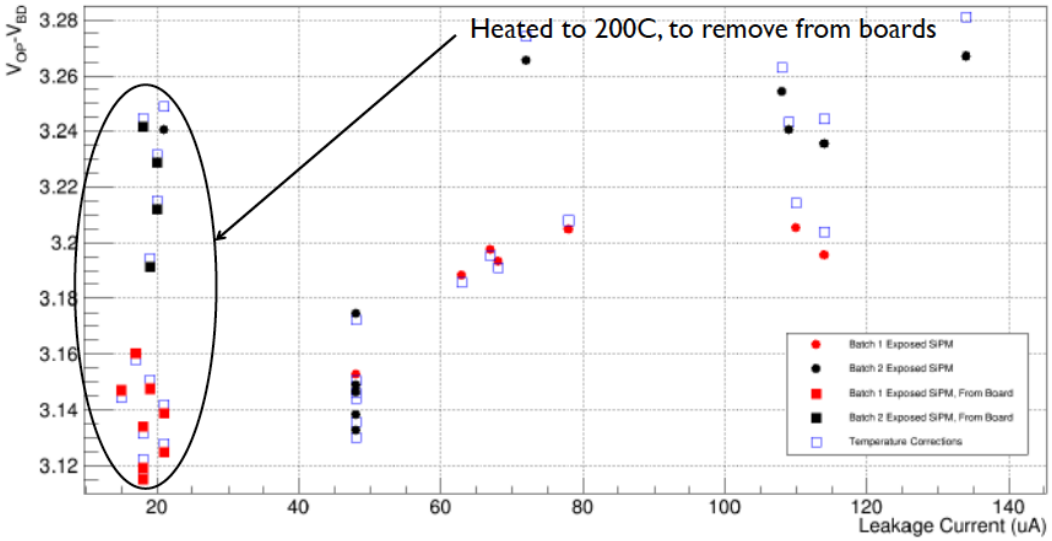

Figure 1.7. Changes in Vop- Vbd vs leakage current.

Additional tests were performed to check if heating of the junction due to increased current may be responsible for changes in response within the limited range accessible experimentally. SiPMs were illuminated with a blue LED at 500 kHz, and at the same time, the single pixel response was measured between LED pulses. With an average current ~10 uA, we did not observe any changes in the gain. At higher current levels and with current preamplifiers, reliable extraction of the gain was problematic.

Finally, we measured the excess noise factor (ENF) due to the degradation of various sensors (SiPM and APDs) for the EMCAL and HCAL modules with cosmic muons. For the EMCAL, we used available PHENIX shashlik modules. For the HCAL, we used a re-designed version of the 2014 UCLA HCAL prototype, where we effectively improved the light collection by a factor of ~3 compare to the 2014 version, and also reduced the number of SiPMs per tower for the readout.

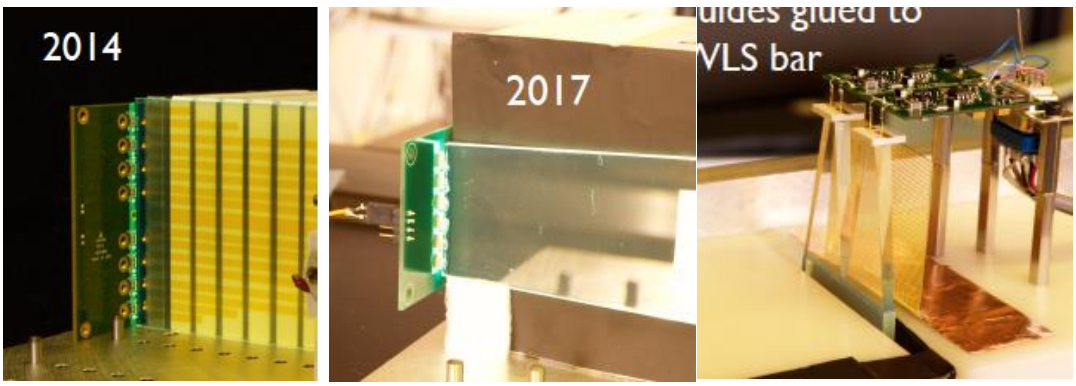

Figure 1.8. HCAL Light collection schemes, SiPMs left and center, APDs (right).

Figure 1.8 shows the old and redesigned version of the light collection schemes for the HCAL, with six SiPMs per tower in the middle and with two APDs readout per tower on the right. For the EMCAL module, we found that with un-exposed SiPMs, the ENF is ~ 1.7 MeV, where the conversion to energy was done using the energy equivalent of a MIP that was measured in the test beam at FNAL in 2016 for this particular EMCAL module. After exposure in Run 17, the ENF grew to 10 MeV.

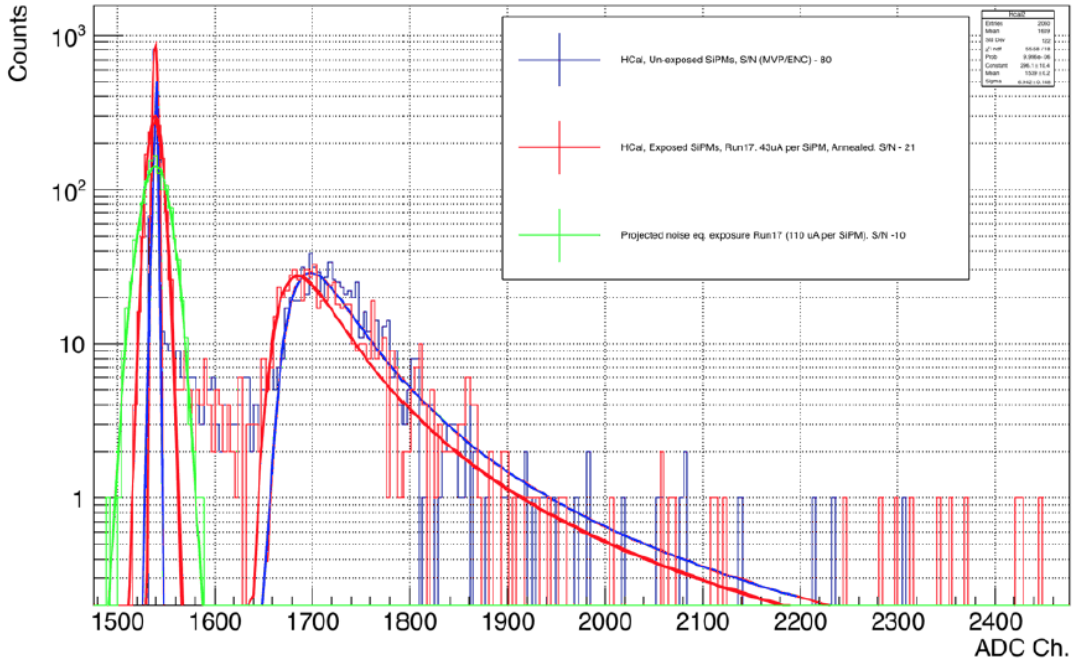

Figure 1.8. Muons in HCAL, exposed and un-exposed SiPMs.

For the HCAL, we defined the S/N as a ratio of the MPV of the Landau peak to the width of the pedestal to compare the performance of exposed and un-exposed SiPMs and APDs. For the SiPMs, the absolute calibration of the readout chain was performed using the single pixel response, while for APDs, the absolute calibration was done with a Fe55 source. To give the ENF in MeV for HCAL we used a GEANT4 prediction for the energy equivalent of a MIP to GeV.

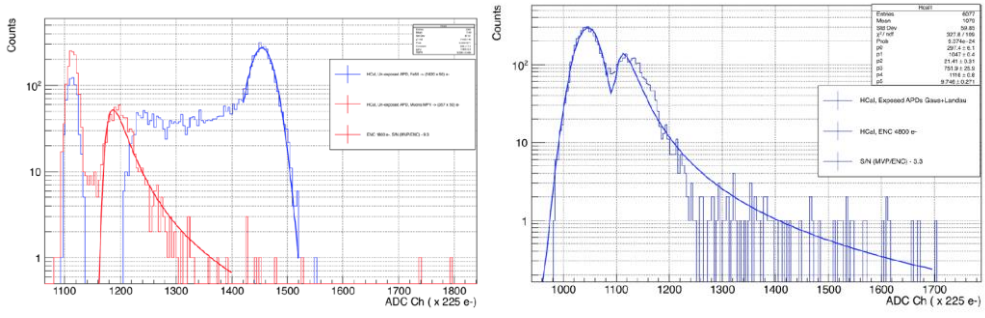

Figure 9. HCAL APD readout. Calibration with Fe55. MIP un-exposed sensors (left), exposed (right).

The response of the HCAL to cosmic muons with the SiPM readout is shown in Figure 1.9. For un-exposed sensors, the S/N is close to 80 (blue spectra in Fig 1.9). We used six exposed SiPMs, which had leakage current after exposure at about 110 uA per sensor. According to our electronics shop, mounting them to the readout board

required heating them to about 200 C for a short period of time, which had a strong annealing effect resulting in decreased leakage current per SiPM to 43 uA (red spectra in Fig 1.9). The slight shift of the MPV to a lower value may be due to misalignment of the sensors with respect to WLS during gluing or due to degradation of the response discussed earlier in this report. The S/N for exposed sensors is close to 20. Without annealing, the S/N would be at around 10. In the case of the APDs, we found that the S/N for un-exposed sensors is close to 10 and in case of exposed sensors, the S/N drops to ~3 as shown in Figure 1.10.

For the SiPM readout, the ENF is approximately 100 MeV per tower for exposures close to the one observed in Run17. For illustration, an ENF of 100 MeV in a single tower will add an additional ~400 MeV to a resolution of ~ 8 GeV for a single hadron at 100 GeV, assuming a 4 x 4 tower cluster size.

It is important to note that the APDs used for these tests are standard HPK S8664-55 APDs. They lack a perimeter groove compared to the CMS and PANDA versions, which can significantly reduce the leakage current with exposure. The 5x5 mm^2 active area is also not optimal, and required us to add additional light guides as shown in Fig 1.8 with additional losses in light collection. In the case of optimized APDs for our geometry (2.9 x 14 mm^2) with a perimeter groove, the S/N would be close to that which was measured with SiPMs. However, as we discussed in our previous reports, due to the Nuclear Counter Effect (NCE) in APDs, one would need to double the number of readout channels (i.e. have an independent readout channel for every APD). **For these reasons, we think that the future development/refinement of the readout schemes for sampling calorimeters at EIC should concentrate on SiPMs. We believe that for any design, one should take into account the fact that SiPMs will degrade in performance with EIC running conditions, and that each SiPM could have different characteristics. A pre-selection of SiPMs will be a necessary step in the construction of any actual calorimeter.**

Future Plan.

We will investigate in detail how Vbd changes with exposure. All characterised SiPMs will be exposed one more time during Run 18 and their characteristics will be re-measured. We also want to get a better understanding of the annealing effects and investigate if an ‘active’ annealing scheme can be implemented practically in order to slow down the degradation of the performance of SiPMs with exposure.

Manpower.

Almost all of the measurements, analysis of data, automation of measurements etc. were made by UCLA students M.Warner, M.Sergeeva, D.Neff and visiting student Hu Yu from Fudan University. We expect to continue to employ many students in our R&D project in FY2018.

Sub Project 2: Progress on Tungsten Powder Calorimeter R&D at BNL
Project Leader: C.Woody

Past

What was planned for this period?

Our main activities for this period were:

- Complete our study of the light guides that will be used in our next prototype calorimeter and which will hopefully be used in the final sPHENIX detector.
- Complete the construction of our new v2.1 prototype calorimeter that will contain new 2D projective W/SciFi blocks, light guides and readout electronics and prepare to test it at Fermilab in early 2018.
- Complete the analysis of our test beam results from our 2016 and 2017 tests and submit them for publication.
- Write up our results on our study of radiation damage in SiPMs and submit them for publications.

What was achieved?

Light Guide Study

We completed our study of various types of light guides and decided on a final design for our prototype calorimeter. This included simulation studies using the ray tracing program TracePro as well as numerous measurements in the lab with various forms of light guide prototypes. Figure 2.1 shows some of the ray tracing results from TracePro. The figure on the left shows the paths of light rays through a 25 mm long trapezoidal light guide and onto the SiPM readout surface. The input fiber is located in the lower right corner. The plot on the right shows the irradiance map, which gives a quantitative distribution of the incident rays onto the 4 SiPMs.

Numerous light guide geometries were studied using these simulations, including various types and shapes of Winston cones and other geometries. A summary of all of these results was presented at the 2017 IEEE NSS/MIC conference in Atlanta in October, 2017 and will be included in the Conference Proceedings. The most dramatic revelation from this study was the fact that most rays bounce at most once on the surface of the light guide before reaching one of the SiPMs. This effect did not depend significantly on the geometry of the light guide, and is mainly due to the narrow exit angle of the light leaving the fiber and the shortness of the light guide. It tells us that such a short light guide is a very poor mixer of the light leaving the fibers, and also explains why various treatments of the light guide surface do not have a large effect on the overall light collection efficiency or uniformity. It also explains why we have observed a strong position dependence in the energy response across a given tower in our test beam results. Since this is really a fundamental limitation imposed by the requirement that we must use a very short light guide due to space constraints inside the sPHENIX magnet, this is not an easy problem to overcome, and there will almost surely be some position dependence to the energy response of the final calorimeter, leading to a worsening of the energy resolution.

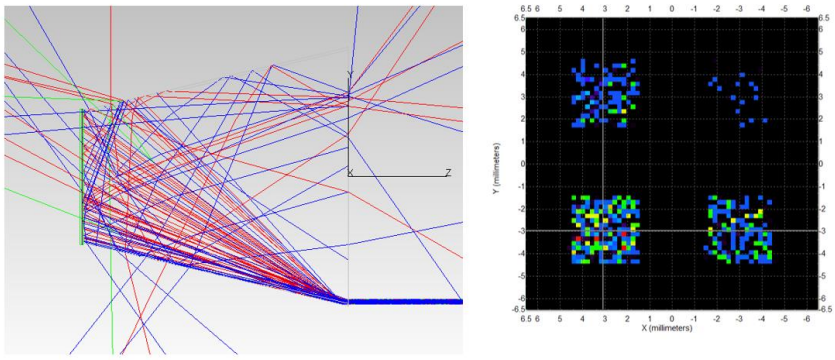

Figure 2.1. Light guide simulation using TracePro. The ray tracing on the left shows the paths of light rays through the light guide and onto the SiPM readout surface. The input fiber is located in the lower right corner. The plot on the right shows the irradiance map, which gives a quantitative distribution of incident rays onto the 4 SiPMs

For the lab measurements, the uniformity is measured by scanning a single, LED-pulsed fiber across the input surface of the light guide while measuring the light collected at the readout surface by either the SiPMs or a PMT. The full coverage PMT measurement gives a *best case* light collection measurement for comparison. The efficiency then is defined as the amount of light incident on the SiPM or PMT active area divided by the amount of light entering the light guide.

Figure 2.2 shows a series of scans for a 25 mm trapezoidal light guide using both a PMT and 4 SiPMs compared with simulation results from TracePro (this plot was also shown in our last report but is included again here for convenience). The agreement between the measurements and the simulations are quite good, although the simulations show slightly more variation than the measurements, probably due to other dispersion effects not included in the simulation.

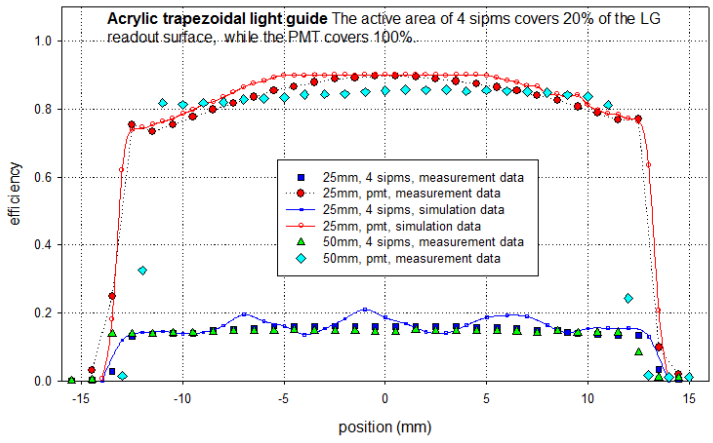

Figure 2.2. Light collection efficiency and uniformity of a 25 mm trapezoidal light guide measured in the lab with a PMT covering the entire readout end and with 4 SiPMs. The results are compared to a Monte Carlo simulation using TracePro.

The conclusion from this study was that a simple trapezoidal light guide gave the best overall performance in terms of light collection efficiency and uniformity, and was the simplest to make. Longer light guides yielded only a slight improvement in the uniformity, but would require additional space inside the magnet to implement, which is not really an option for sPHENIX. These results were also confirmed by the measurements of our prototype calorimeter in the test beam earlier this year, as described in our previous report in July 2017. We therefore decided to use 1" trapezoidal light guides for our next prototype detector, and which will also hopefully be used for the final calorimeter.

We then proceeded to order injection molded trapezoidal light guides from a company that specializes in precision injection molded parts (NN Inc, which is a Division of Precision Engineering Products located in Providence, Rhode Island). They use a highly polished mold to produce the parts and use a carefully controlled process to cool the part after extrusion to avoid voids and distortions in finished material. We worked with them to improve the casting of the parts and just recently obtained the first samples, examples of which are shown in Fig. 2.3, and they look extremely good. These light guides look essentially as good as the individually machined light guides that we used in our previous prototype, but cost only ~ $3 a piece in large quantities (~ 25K total light guides for the sPHENIX calorimeter).

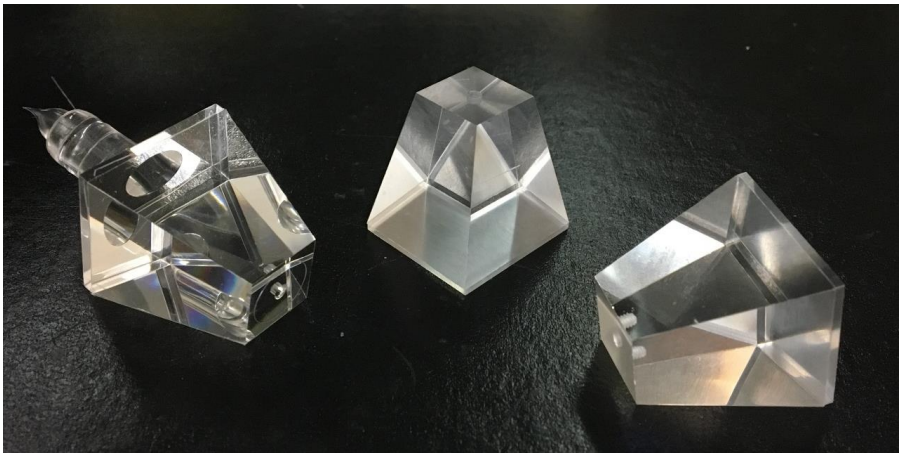

Figure 2.3. Injection molded acrylic light guides for the v2.1 prototype calorimeter produced by NN Inc (a Division of Precision Engineering Products). The part on the left is as received, which requires machining off the sprue and the other flat end and tapping the mounting hole for the SiPM readout board. The parts on the right are the finished light guides.

Construction of a new 2D Projective Calorimeter Prototype

As described in our previous report in July, we tested our first 2D projective calorimeter prototype (which we call the v2 prototype) in Jan-Feb 2017 at Fermilab. The results showed a strong position dependence to the energy response for electrons, which was partially due to the non-uniformities in the light collection from the light guides as described above, but also due to inefficiencies and dead areas around the boundaries between blocks. This was mainly due to the fact that the blocks that were tested were the first 2D projective blocks ever made, and significant improvements have been made in producing these blocks since that time.

Figure 2.4 shows the new set of sixteen 2D projective blocks produced at UIUC that will be used in our new v2.1 prototype calorimeter. This prototype will consist of 16 absorber blocks that are representative of the sPHENIX calorimeter at large rapidity ($\eta \sim 1$). As in our previous prototype, each block contains 2x2 towers which are each individually read out with their own light guide. The quality of these blocks is significantly better than those used in the previous prototype. The apparent dead regions around the boundaries of the blocks are due to the fact that the fibers are tapered inward towards the center at the readout end, which helps improve the light collection at the block boundaries, and also allows us to use the same light guide for all blocks. The optical quality of the readout end is also quite good, and there are very few dead or missing fibers. We have also developed a testing procedure to measure the number of good fibers at the readout end that will be used for quality assurance for all the final production blocks. Figure 2.5 shows an example of the results of this testing procedure which gives the fraction of good fibers in each quadrant (corresponding to a single tower) relative to the expected number as a figure of merit.

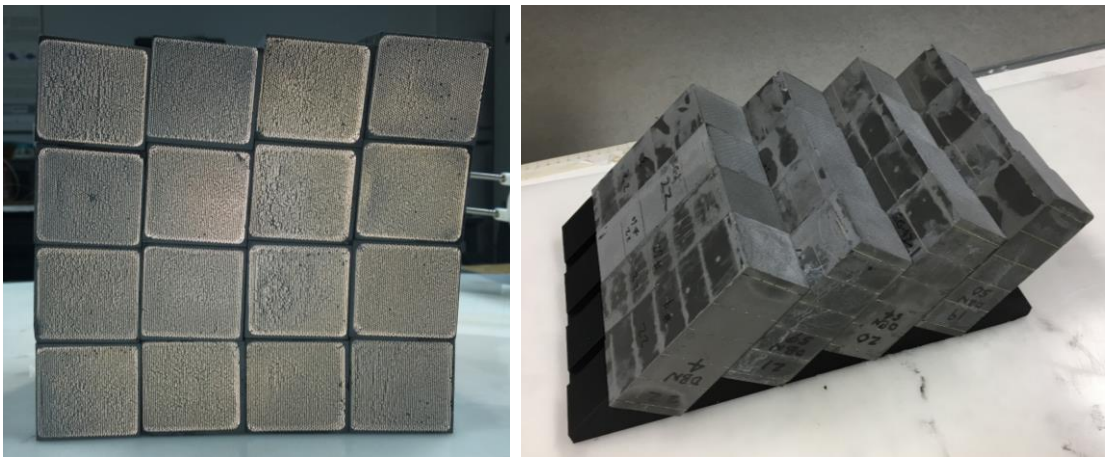

Figure 2.4. New 2D projective blocks produced at UIUC for the v2.1 prototype that will be tested at Fermilab in Feb-Mar of 2018. The dead areas around the edges of the blocks are due to the fact that the fibers are tapered inward towards the center of the block at the readout end. The photo on the right shows the blocks being test fitted into their mounting support.

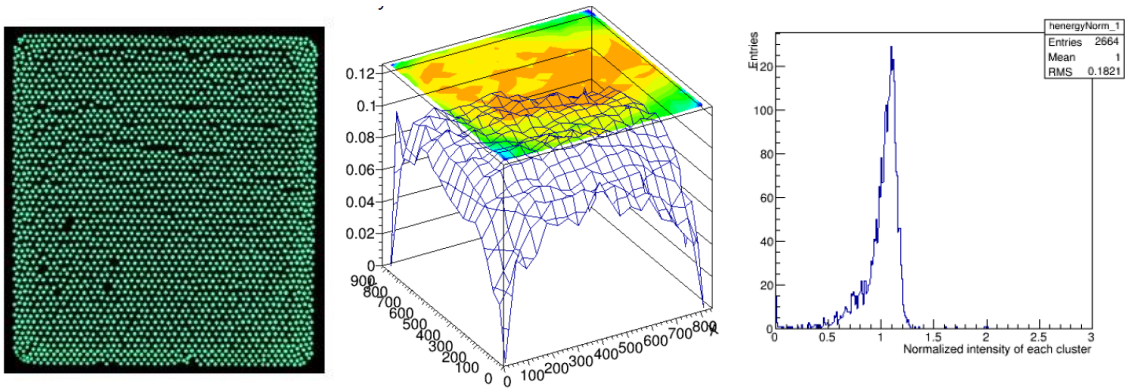

Figure 2.5. Left: Optical image of the readout end of a block used for fiber scanning; Middle: Uniformity map of fibers within a block; Right: Distribution of normalized light intensity of fibers within a block used as a figure of merit for quality control.

Figure 2.6 shows the mounting frame, or “sawtooth”, that will be used to support the blocks within the v2.1 prototype. It will utilize the same mounting system that we plan to use in the final sPHENIX detector. The blocks are first glued together into modules consisting of 4 blocks corresponding to a ϕ or η slice of a sector, and then the modules are glued to the sawtooth support. The entire assembly is then installed in the metal enclosure shown on the right, which allows for cables, electronics and cooling to be brought out at one end.

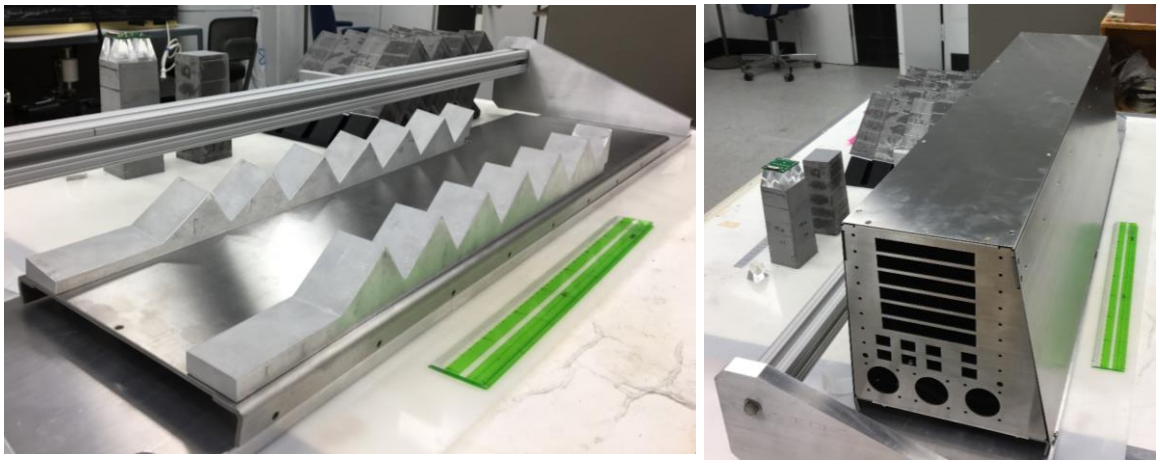

Figure 2.6. Mechanical assemblies for the v2.1 EMCAL prototype.

Figure 2.7 shows the SiPM readout boards for the v2.1 prototype. Each readout board consists of four groups of 2x2 arrays of SiPMs (one array for each tower) that will be mounted onto one block with its four light guides. These readout boards are then connected to preamp boards with short cables, which are then connected to interface boards that bring the signals through cables to the end of the detector, as shown in Fig. 2.6. The v2.1 also utilizes a complete water cooling system for the SiPMs and preamp electronics, similar to what will be used in the final sPHENIX detector.

Figure 2.7. SiPM readout boards and readout electronics being prepared for installation on the v2.1 prototype.

What was not achieved, why not, and what will be done to correct?

We again essentially achieved all that we planned to do during the past six months. The delivery of the light guides was delayed due to various procedural requirements by sPHENIX needed before we could place the order for the light guides, which caused 6 week delay. After several first iterations by the manufacturer, they finally arrived in mid December, which has resulted in a very tight schedule for completing the final assembly and testing of the prototype in order to get it ready to send to Fermilab in mid February. We nevertheless feel that we will make this schedule in order to get the detector to Fermilab in time for the beam test.

As far as publications, we completed our analysis of the 2016 and 2017 test beam data and submitted them for publication as planned. We did not finish writing up our results on radiation damage in SiPMs, but we hope to complete this in early 2018.

Future

What is planned for the next funding cycle and beyond? How, if at all, is this planning different from the original plan?

Our main activity during the next six months will be to carry out the beam test of the v2.1 prototype at Fermilab and to analyse the test beam data. We also plan to start fabricating the blocks for one complete sector of the sPHENIX EMCAL, which we call the Sector 0 preproduction prototype. This will allow us to establish the production procedure for all the final blocks, as well as the procedures for fabricating modules from these blocks and assembling them into sectors. After establishing these procedures, we plan to produce 12 additional preproduction sectors in order to fully qualify the factories at UIUC and BNL for producing the remaining sectors for sPHENIX. Building and testing the v2.1 and first preproduction sector has always been in our original plan, but the production of the 12 preproduction sectors is a new addition to our plan since the last period.

What are critical issues?

The most critical issues during the next six months will be to measure the performance of the v2.1 prototype and characterize its performance, and to start to build the first preproduction sector for sPHENIX. The performance of the v2.1 will essentially define the performance of the final sPHENIX detector, and the procedures developed for producing Sector 0 will become the procedures used for all the remaining sectors in sPHENIX.

Manpower

Include a list of the existing manpower and what approximate fraction each has spent on the project. If students and/or postdocs were funded through the R&D, please state where they were located, what fraction of their time they spend on EIC R&D, and who supervised their work.

The effort on the sPHENIX EMCAL is being carried out mainly by the BNL sPHENIX Group and the group at UIUC, with additional input and support from the groups at the University of Michigan and Debrecen University in Hungary.

External Funding

Describe what external funding was obtained, if any. The report must clarify what has been accomplished with the EIC R&D funds and what came as a contribution from potential collaborators.

The effort on the sPHENIX EMCAL is being supported entirely by external funds. There is no support for these activities from EIC R&D funds.

Publications

Please provide a list of publications coming out of the R&D effort.

Our paper on our test beam results from 2016, "Design and Beam Test Results for the sPHENIX Electromagnetic and Hadronic Calorimeter Prototypes", was revised after its first review and resubmitted to the IEEE Transactions on Nuclear Science in September 2017. It is currently waiting for its final review and approval for publication.

A paper on our 2017 test beam results, "Test Beam Results and Status of the sPHENIX Calorimeter System", was submitted to the IEEE Conference Record for the 2017 IEEE Nuclear Science Symposium and Medical Imaging Conference in November 2017.

A paper on the study we carried out on the light guides, "Light Collection Efficiency and Uniformity of Light Guides for the sPHENIX Electromagnetic Calorimeter", was submitted to the IEEE Conference Record for the 2017 IEEE Nuclear Science Symposium and Medical Imaging Conference in November 2017.

A paper on our studies of radiation damage in SiPMs, "Results of the Effects of Neutron and Gamma Ray Irradiation on Silicon Photomultipliers", is currently in the final stages of preparation and will be submitted to the IEEE Transactions on Nuclear Science in early 2018.

Sub Project 3: Development of a High Density, Fully Projective Shashlik Electromagnetic Calorimeter with Improved Energy, Position and Timing Resolution for EIC
Project Leaders: S. Kuleshov and E. Kistenev

Past

What was planned for this period?

- Production of a single tower technological prototype: July-September 2017
- Production of 3x3 towers rectangular prototype: July-December 2017
- Production of hodoscopes: July-December 2017
- Production of read out for hodoscopes: July-October 2017
- Production or purchase of the readout for calorimeters: July-November 2017

What was achieved?

1. The scintillator plastic tiles for the shashlik prototype with spiral fibers with dimensions of 38 x 38 x 1.5 mm size were bought and delivered to UTFSM.
2. 900 38 x 38 x 1.5 mm W80Cu20 plates were bought and delivered in UTFSM.
3. 80WCu20 plates were covered with 70 micron thick white vinyl film (Metamark).
4. CAD/CAM design of the plates was completed
5. Drilling of holes in 300 plates is under production
6. 100 MPPCs for the calorimeter were ordered and paid for
7. We are working on the design of power supplies and read out electronics
8. The hodoscope was designed, constructed and tested during NA64 run at CERN

What was not achieved, why not, and what will be done to correct?

Progress on this project is greatly limited due to limited manpower and lack of funding from EIC R&D.

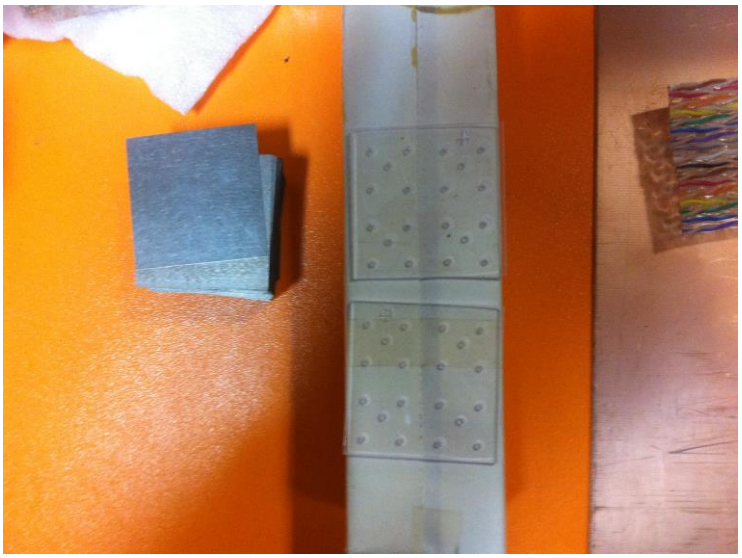

Fig. 3.1 38 x 38 x 1.5 mm W80Cu20 plates and the scintillator plastics for the shashlik prototype with spiral fibers.

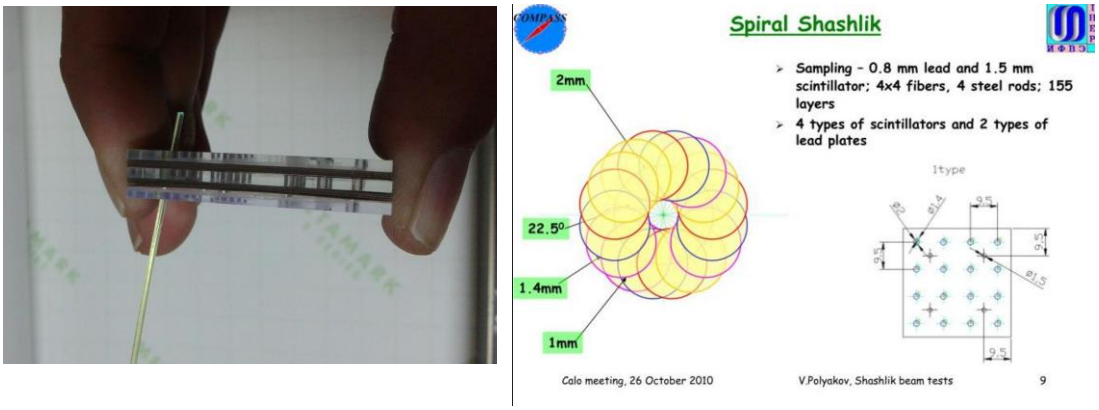

Fig. 3.2 Design of the spiral channel in the calorimeter module.

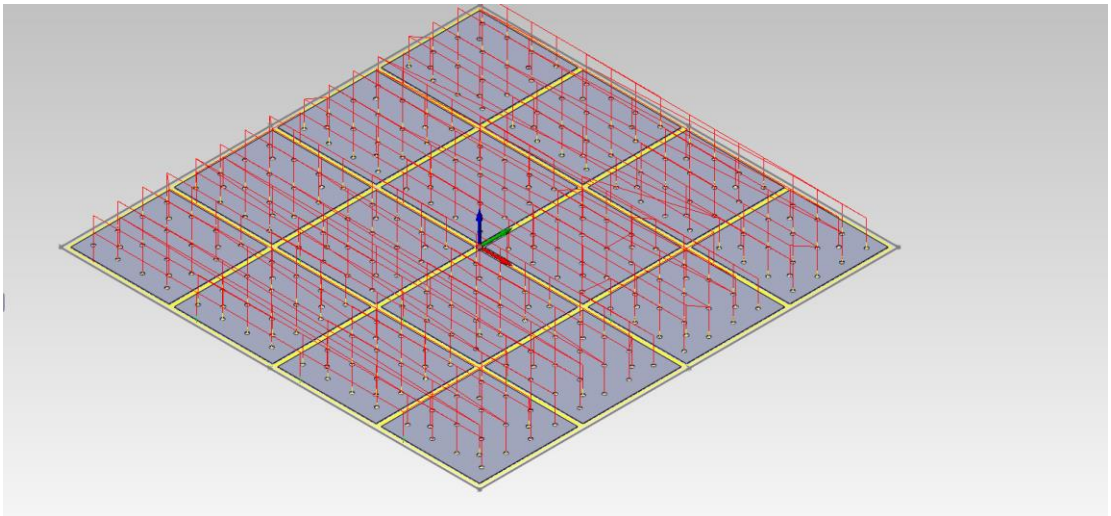

Fig. 3.3 CAD/CAM design of 80WCu20 plates for machining

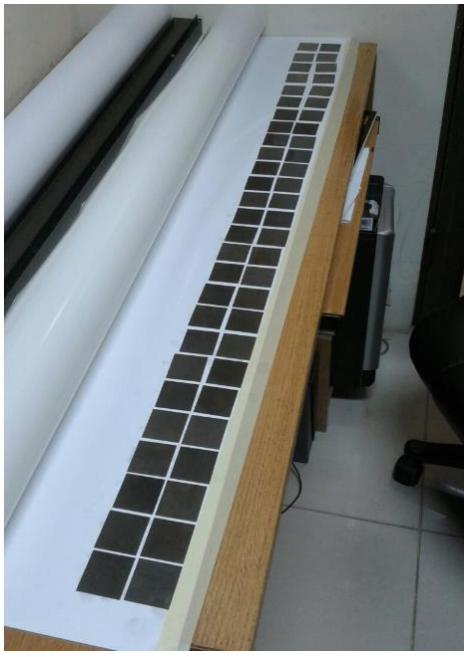

Fig. 3.4 Depositing optical white reflector on 80WCu20 plates (70 micron thick white vinyl film from Metamark)

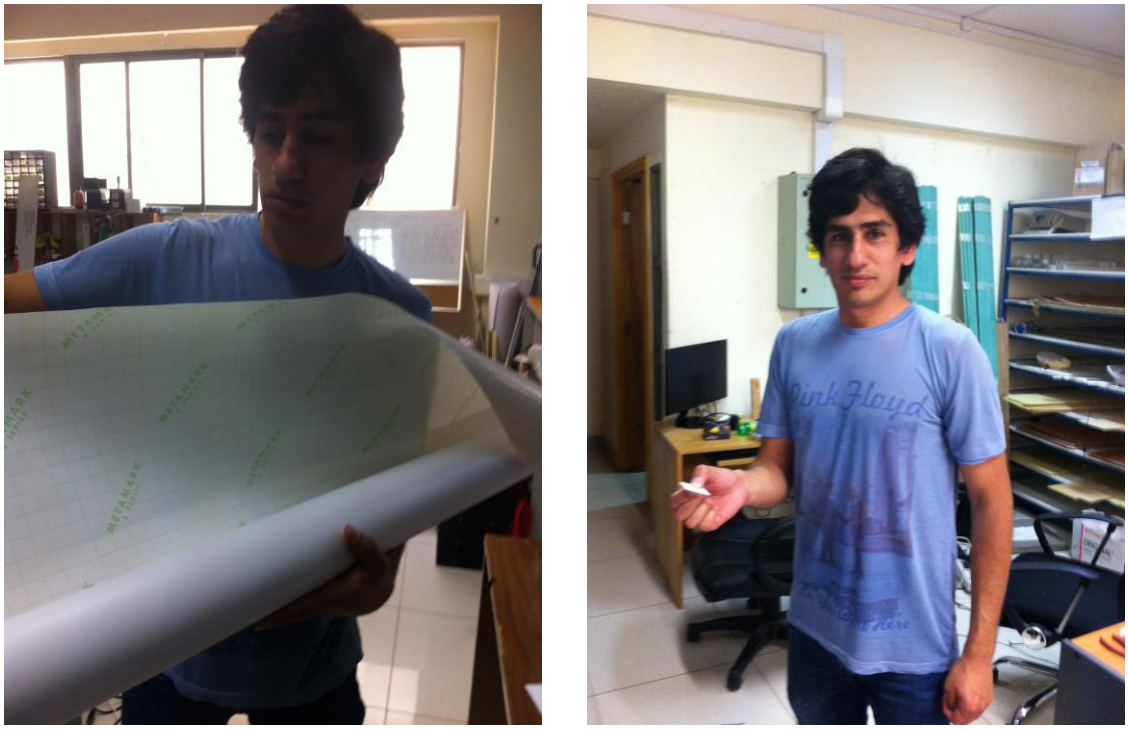

Fig 3.5. A mechanical engineer, Eliás Rozas, works on the project

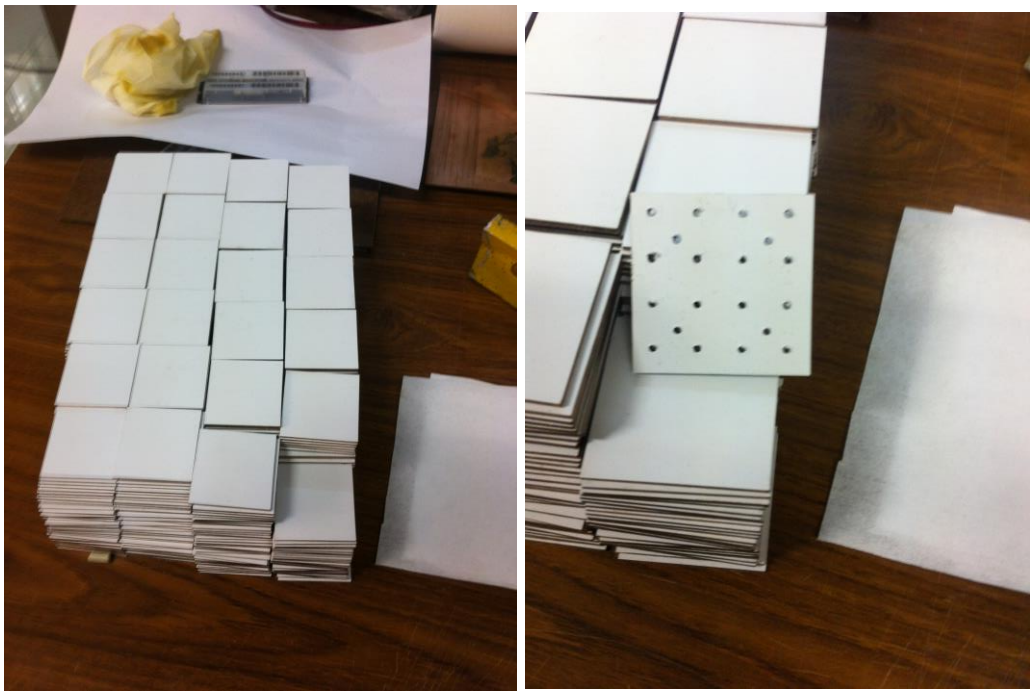

Fig. 3.6. 80WCu20 plates with white optical reflector.

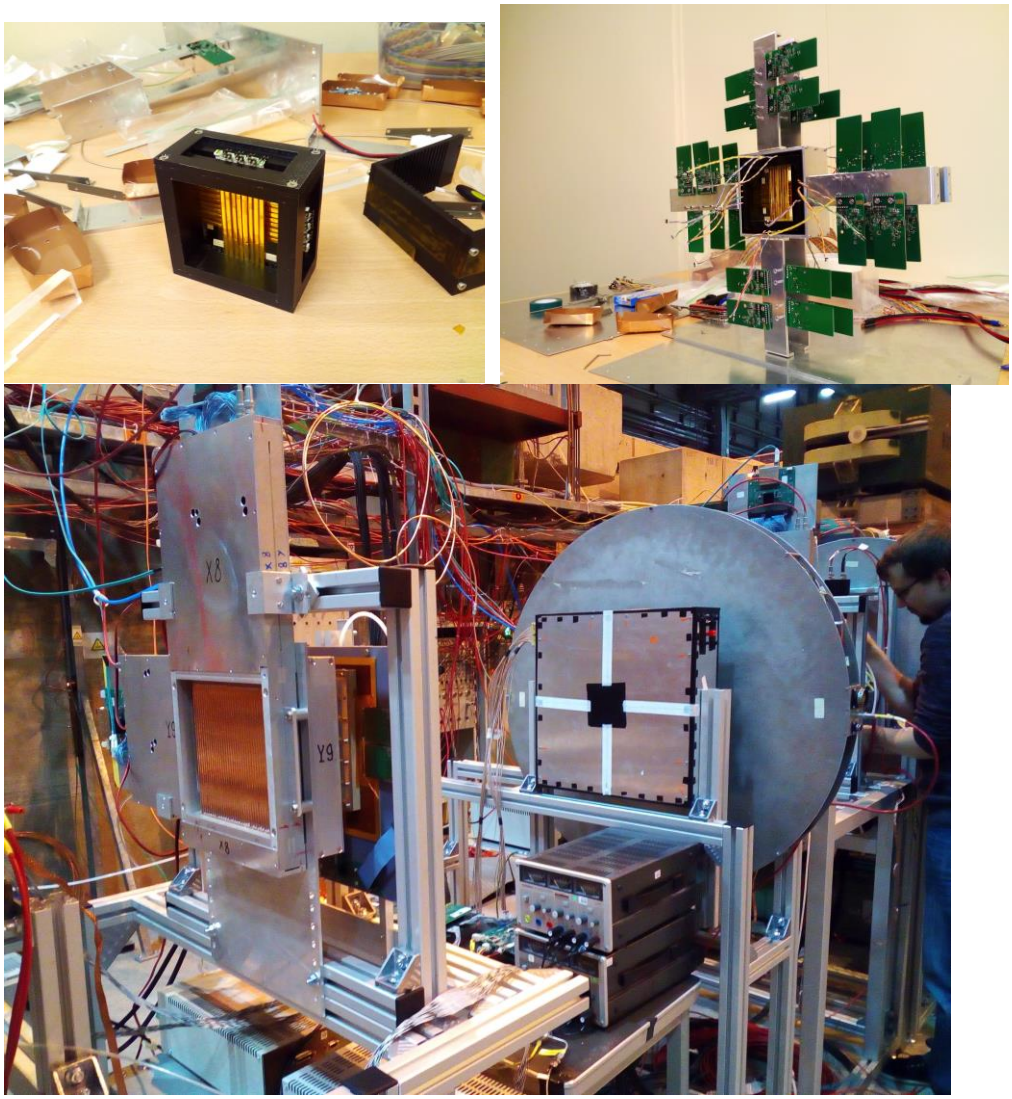

Fig. 3.7. Hodoscope at beam area of NA64.

Future

What is planned for the next funding cycle and beyond? How, if at all, is this planning different from the original plan?

UTFSM plans to produce 1 module with 40 X0 and 1 module with 20 X0. We plan to test the 40 X0 module in the test beam at CERN in May of next year, and the 20 X0 module will be tested in the Detector Laboratory at UTFSM.

What are critical issues?

We need to know if additional funding will be provided by EIC Detector R&D to support this project.

Additional information:

Manpower

Include a list of the existing manpower and what approximate fraction each has spent on the project. If students and/or postdocs were funded through the R&D, please state where they were located, what fraction of their time they spend on EIC R&D, and who supervised their work.

- A mechanical engineer, Eliás Rozas, works on the project (70% time) from June.
  A postdoc, Pablo Ulloa, works on the project (30% time) from July.
  An electronic engineer, Lautaro León works on electronics for the modules (30% time).
- Technicians and engineers are covered by the Detector Laboratory at UTFSM through the New Small Wheel upgrade of the ATLAS Experiment
- None of the personnel working on this project were funded through EIC R&D.

External Funding

Describe what external funding was obtained, if any. The report must clarify what has been accomplished with the EIC R&D funds and what came as a contribution from potential collaborators.

This work is being done completely with internal funding of the Detector Laboratory of UTFSM. There is currently no support from EIC Detector R&D for this project.

Publications

Please provide a list of publications coming out of the R&D effort.

Sub Project 4: Crystal Calorimeter Development for EIC based on $PbWO_4$
Project Leader: T. Horn

Past

What was planned for this period?

- ***Crystal characterization for crystal specification and impact on EIC detector performance, e.g. on the constant term***
    - Characterize, including chemical analysis, 300-400 SICCAS crystals produced in 2017 in collaboration with the NPS project
    - Evaluate influence of crystal surface properties
    - Evaluate crystal-to-crystal variation of higher crystallization Crytur crystals, which are expected to have higher impurity concentrations
- ***Construct a prototype to establish limiting energy and position resolution, and, together with simulations and crystal characterization, explore options to reduce the constant term***.
    - Use the prototype together with simulations to evaluate contributions to the overall resolution and reducing the constant term including uniformity of crystal response and statistical fluctuations of containment losses.
    - Establish actual energy and position resolution in test beam.
- ***Investigate different readout systems and influence on the constant term***
    - Investigate different readout options with the prototype.

What was achieved?

With commitment of internal university and laboratory funds and through synergy with the NPS project at JLab we managed to partially carry out crystal characterization at CUA and IPN-Orsay for crystal specifications and impact on EIC detector performance. Our activities are listed below. Please refer to the appendix for additional information.

- Procured components and allocated space for crystal characterization at both CUA and IPN-Orsay
- Established a non-destructive sampling method for chemical composition analysis
- Performed chemical composition and surface analysis, and tested the optical properties of 120/320 crystals produced at SICCAS in 2017 that were procured through synergy with the VSL and the NPS project.
- Provided feedback to vendors and iterating on reaching required crystal properties and quality, e.g. by “compensation” of the crystal surface.

What was not achieved, why not, and what will be done to correct?

The *actual* FY17 budget some of us started receiving in November 2017 was cut by 65% from the requested budget. As stated in our July 2017 report, in the case of a 40% cut from the requested budget, we would not be able to continue our crystal characterization studies. Our focus would mainly shift towards the NPS project, which would be the funding source for these activities, and we may only provide information relevant specifically for EIC. We would attempt to continue our general studies of different readout options at lower efficiency. These would proceed at significantly reduced efficiency regarding EIC. Construction and testing of the prototype is delayed. Our work in this period is commensurate with our July 2017 statement. No corrective actions are anticipated or needed.

Future

What is planned for the next funding cycle and beyond? How, if at all, is this planning different from the original plan?

For the remainder of the funding cycle we plan to make our best effort to complete our goals from the previous FY17 cycle and also try to make progress beyond that as budget constraints allow. Our highest priority is to determine ways to reduce the constant term, which includes nonlinearities in light collection that are in part properties of the crystal itself. To achieve this we plan to:

- Continue crystal characterization including optical, chemical composition and surface studies for additional samples
- Measure radiation hardness of crystals and investigate correlations with chemical composition
- Iterate with vendors on crystal requirements and composition optimization, e.g. surface and chemical composition.
- Procure, in collaboration with the NPS project, rectangular crystals from CRYTUR
- Attempt to continue our general studies of different readout options.
- Construct a prototype to test if actual crystal performance is suitable for EIC.

What are critical issues?

At this stage, the most critical issues are to complete the FY17 activities and explore options to reduce the constant term. Crystal characterization including optical, chemical composition and surface studies and prototyping for actual crystal performance are critical, as well as iterations with vendors, e.g. Crytur, with the goal to develop the ability to produce PbWO4 crystals suitable for EIC.

Additional information:

Manpower

Include a list of the existing manpower and what approximate fraction each has spent on the project. If students and/or postdocs were funded through the R&D, please state where they were located, what fraction of their time they spend on EIC R&D, and who supervised their work.

IPN-Orsay
M. Josselin
Ho San, graduate student
R. Wang, postdoc
G. Hull
C. Munoz-Camacho

CUA
S. Ali, graduate student
D. Griggs, high school
S. Roustom, high school
R. Trotta, graduate student
A. Vargas, graduate student
V. Berdnikov, postdoc
T. Horn
I. Pegg
Vitreous State Laboratory

Yerevan
H. Mkrtchyan
V. Tadevosyan
A. Asaturyan

BNL
C. Woody
S. Stoll
M. Purschke

Caltech
R-Y Zhu

External Funding

Describe what external funding was obtained, if any. The report must clarify what has been accomplished with the EIC R&D funds and what came as a contribution from potential collaborators.

- All of the FTEs required for working towards finalizing the crystal test setup and crystal characterization are provided by CUA/VSL/IPN-Orsay or external grants. The absence of any labor costs makes this proposed R&D effort extremely cost effective.

- The 2014 and 2015 SIC crystals, as well as 460 SIC crystals produced in 2017 are provided through synergistic activities with independent research for the Neutral Particle Spectrometer (NPS) project at JLab.

- The expertise and use of specialized instruments required for crystal characterization and their chemical analysis, as well as additional crystals samples are made possible through collaboration with the Vitreous State Laboratory (VSL) at CUA that is also collaborating on the NPS project.

Efforts related to crystal studies as described here were accomplished with external funds through synergistic activities with the NPS project at JLab. Additional funds and facilities for crystal characterization were provided by the Vitreous State Laboratory at CUA. Salaries and wages were provided by private external grants from the individual principal investigators, e.g., IPN-Orsay, Yerevan, and the National Science Foundation.

Publications

Please provide a list of publications coming out of the R&D effort.

C. Munoz-Camacho et al., "*R&D for high resolution calorimetry at the future Electron-Ion Collider*", Presentation at the XVIIth International Conference on Calorimetry in Particle Physics, 15-20 May, 2016, Daegu, South Korea

Through synergy with the NPS project at JLab:

R. Trotta et al. "*Exclusive reactions and the PbWO4-based Inner Calorimeter for the Electron-Ion Collider*" presentation at the APS April 2017 meeting, Washington, DC

T. Horn, C. Munoz-Camacho, C. Keppel, I. Strakovsky et al., arXiv:1704:00816 (2017) "*Workshop on High-Intensity Photon Sources (HIPS2017) Mini-Proceedings*"

T. Horn et al., J.Phys. Conf. Ser. **587** (2015) 1, 012048 "*A PbWO4-based Neutral Particle Spectrometer in Hall C at 12 GeV JLab*"

T. Horn et al. "*Physics Opportunities with the Neutral Particle Spectrometer in Hall C*", presentation at the APS DNP 2015 Fall meeting, Santa Fe, NM

APPENDIX:

PbWO4 crystal characterization

At CUA, both chemical composition plus surface analysis and optical measurements (transmittance, light yield), as well as radiation resistance studies were carried out. About half of 320 crystals manufactured by SICCAS in 2017, 45 crystals manufactured by SICCAS in 2014 and 201, and 3 crystals from CRYTUR received in 2017 were characterized. Correlation studies between chemical composition and surface and optical properties/radiation hardness were evaluated and communicated to the vendors.

The surface analysis was performed with a scanning electron microscope with EDS and WDS systems and nanomanipulator (JEOL 6300, JEOL 5910) and in collaboration with the VSL. Figure A.1 shows the typical surface quality of crystals from Crytur at 50um, and BTCP and SICCAS at 500um. The surface of the Crytur crystal is well-polished with negligible mechanical flaws. The BTCP crystal surface has scratches, which is expected as this crystal has been shipped between different institutions multiple times without re-polishing. The SICCAS crystals typically arrive with long scratches on the surface, but also other flaws as shown. In studies of the optical properties it was found that scratches applied in a well-defined manner may actually benefit crystal properties, e.g. the light yield. Discussions with the vendors have started and a procedure is being developed to implement such a surface treatment consistently.

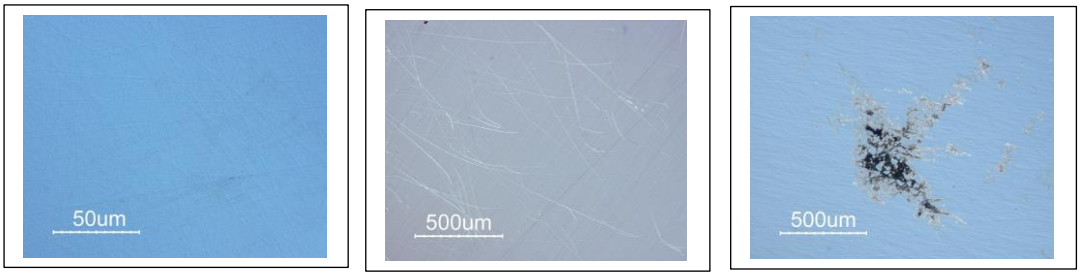

(a) (b) (c)

Figure A.1: Microscope surface analysis of $PbWO_4$ crystals from (a) Crytur, (b) BTCP, (c) SICCAS (produced in 2017)

Looking even deeper into the crystal defects of the SICCAS crystals reveals another correlation with optical properties as shown in Fig. A.2. A fraction of the crystals that pass the light yield and transmittance requirements have bubbles and deep pits up to 20um inside the bulk. The size of these bubbles can be on the order of 100um. These flaws result in an observed very high, but position dependent light yield inducing non-uniformities that negatively impact the resolution requirement for EIC. Discussions with the vendor are ongoing to mitigate these flaws.

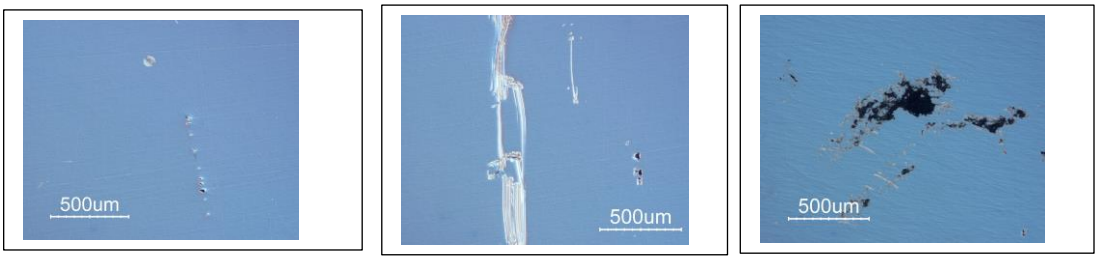

(a) (b) (c)

Figure A.2: Microscope images of bubbles (a), deep scratches (b) and pits (c) observed in SICCAS crystals produced in 2017.

PbWO4 crystal chemical analysis – XRF studies

Chemical composition analysis was carried out at CUA using XRF chemical analysis instrumentation, specially configured for small samples. Samples on the order of 100 microgram were taken from each crystal using a method developed by the VSL. The method is non-destructive and does not impact the crystal optical properties. The latter was verified with dedicated measurements. Approximately 10-15% of the crystals, which were also characterized for optical properties, were investigated in this study.

Figure A.3 illustrates a general overview of the variation in composition for a representative set of crystals in terms of the element oxides. "Good" crystals are denoted as those that pass all optical specifications, while "bad" crystals fail all or a large fraction thereof. The two major materials (PbO and WO_3) used in crystal growing are not shown. The variation in these materials among all good and bad crystals is small (0.5-0.7% on average), which one might interpret as differences in optical properties being due to other contributions in the chemical composition (see results of statistical analyses in the next paragraphs) or mechanical features. The results in Figure A.3 suggest that good crystals have a noticeable contribution from iron oxide (green column) and smaller contributions from at most two others. On the other hand, bad crystals have at least three contributions other than iron.

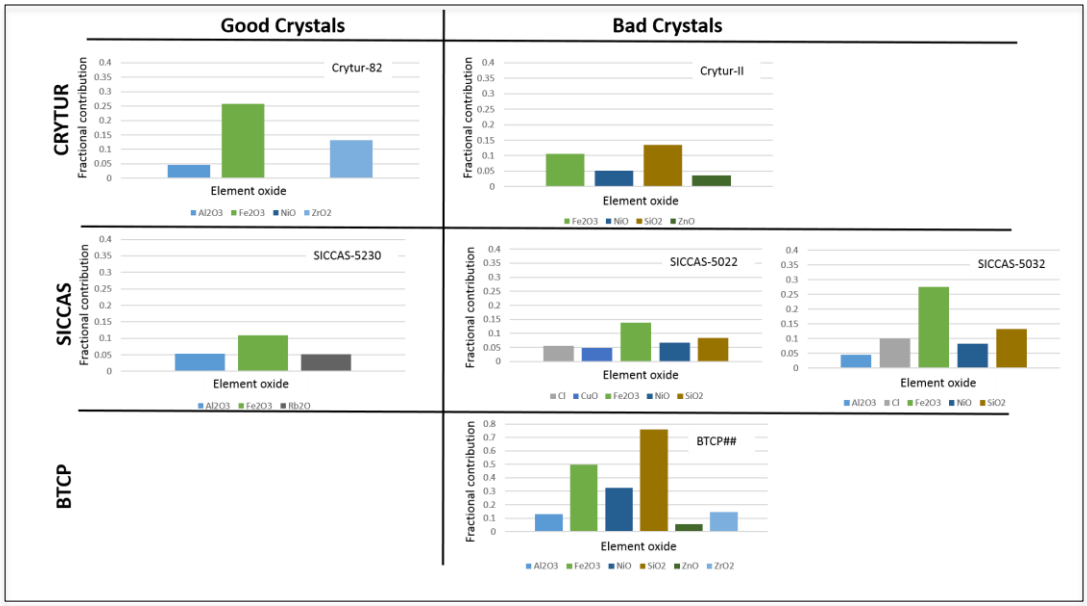

Figure A.3: Crystal composition from XRF analysis. The two major materials (PbO and WO_3) used in PbWO4 crystal growth are not shown.

To investigate the importance of the variation in lead and tungsten oxides, as well as those of the other elements observed in chemical composition analysis, statistical analyses were carried out. The first method is a multivariate approach in which correlations are estimated by a pairwise method. The results are shown in Table 1. A clear dependence of the optical transmittance on the stoichiometry of lead and tungsten oxides can be seen. The light yield does not seem to depend on this stoichiometry.

	Al2O3	CaO	Cl	Cr2O3	CuO	Fe2O3	NiO	PbO	Rb2O	SiO2	WO3	ZnO	ZrO2	Light Yield	LT 420
Al2O3	1.0000	-0.0637	0.0500	0.0222	-0.5035	0.6193	-0.1994	0.2246	0.1136	-0.4142	-0.3617	0.2726	0.2487	0.2094	-0.1775
CaO	-0.0637	1.0000	-0.1947	-0.0910	-0.0910	-0.2581	-0.3309	-0.0255	-0.0910	-0.1440	0.2046	-0.1271	-0.2315	-0.3779	-0.1202
Cl	0.0500	-0.1947	1.0000	-0.1337	0.2209	0.4481	0.6386	0.0721	-0.1337	-0.0945	-0.3613	-0.1868	0.0636	-0.2777	-0.1756
Cr2O3	0.0222	-0.0910	-0.1337	1.0000	-0.0625	0.0620	0.3061	0.3970	-0.0625	-0.2357	-0.3078	-0.0873	-0.1590	-0.2804	-0.4934
CuO	-0.5035	-0.0910	0.2209	-0.0625	1.0000	-0.1440	0.2086	0.2237	-0.0625	0.0827	-0.1630	-0.0873	-0.1590	-0.0919	-0.1861
Fe2O3	0.6193	-0.2581	0.4481	0.0620	-0.1440	1.0000	0.1952	0.4125	-0.2305	-0.4911	-0.7115	0.3980	0.4512	-0.1540	-0.2958
NiO	-0.1994	-0.3309	0.6386	0.3061	0.2086	0.1952	1.0000	0.1406	-0.2273	-0.0730	-0.2637	-0.1491	-0.3345	-0.3974	-0.1615
PbO	0.2246	-0.0255	0.0721	0.3970	0.2237	0.4125	0.1406	1.0000	-0.0700	-0.4356	-0.8960	0.3456	-0.0146	-0.1618	-0.7324
Rb2O	0.1136	-0.0910	-0.1337	-0.0625	-0.0625	-0.2305	-0.2273	-0.0700	1.0000	-0.2357	0.2155	-0.0873	-0.1590	0.0512	0.0207
SiO2	-0.4142	-0.1440	-0.0945	-0.2357	0.0827	-0.4911	-0.0730	-0.4356	-0.2357	1.0000	0.3862	-0.0763	-0.1999	0.2082	0.6228
WO3	-0.3617	0.2046	-0.3613	-0.3078	-0.1630	-0.7115	-0.2637	-0.8960	0.2155	0.3862	1.0000	-0.4071	-0.2302	0.1556	0.6197
ZnO	0.2726	-0.1271	-0.1868	-0.0873	-0.0873	0.3980	-0.1491	0.3456	-0.0873	-0.0763	-0.4071	1.0000	0.1292	-0.2337	0.0767
ZrO2	0.2487	-0.2315	0.0636	-0.1590	-0.1590	0.4512	-0.3345	-0.0146	-0.1590	-0.1999	-0.2302	0.1292	1.0000	0.4764	-0.0142
Light Yield	0.2094	-0.3779	-0.2777	-0.2804	-0.0919	-0.1540	-0.3974	-0.1618	0.0512	0.2082	0.1556	-0.2337	0.4764	1.0000	0.1931
LT 420	-0.1775	-0.1202	-0.1756	-0.4934	-0.1861	-0.2958	-0.1615	-0.7324	0.0207	0.6228	0.6197	0.0767	-0.0142	0.1931	1.0000

Table 1: Multivariate analysis results. A clear dependence of optical transmittance on PbO/WO_3 stoichiometry can be observed. Light yield appears independent of it.

The second statistical method uses partial least squares to construct two correlation models and assess effects of individual variables. The results for two resulting models assessing the impact of chemical composition on light yield and optical transmittance is shown in Figure A.4. Zr, Ni, and Ca seem to be most relevant for light yield, while Si and to a lesser extent Cr seem most relevant for transmittance at 420 nm. The relevance of chemical composition for radiation hardness is currently being investigated. The models will also be tested with additional crystal samples. The focus so far has been on crystals that failed at least one optical crystal requirement.

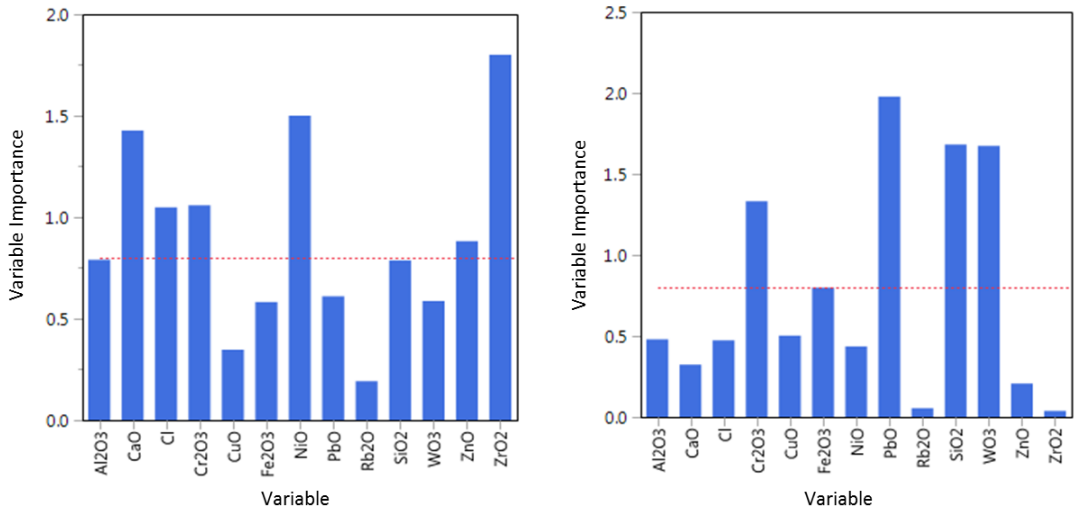

Figure A.4: Effect of individual elements of chemical composition on light yield (a) and optical transmittance (b) based on a partial least squares statistical analysis.

PbWO4 crystal optical studies

At CUA, optical transmittance was measured using PerkinElmer Lambda UV/Vis spectrophotometers with double beam, double monochromator, and a large sample compartment. The spectrometers allow for measurements of the transmittance and absorption between wavelengths of 250 to 2500 nm with 1 nm resolution. The systematic uncertainty in reproducibility of the measurements is on the order of 0.2%. Results for a subset of 50 SICCAS crystals produced in 2017 as a function of crystals ID and for individual crystals as a function of wavelength are shown in Figure A.5. Clear variations in transmittance can be observed, in particular at 420 and 360 nm, where 14% and 20%, respectively, fail specifications. These variations seem to depend on chemical composition (see previous sections). It should be noted that crystals which pass transmittance requirements are not necessarily good crystals. Indeed, 5% of all tested crystals passing transmittance specifications were found to have mechanical flaws resulting in non-uniformities in light collection.

The light yield at CUA was measured with a Photonis XP2262 PMT with a bi-alkali lime glass window. For the light yield measurements, a collimated Na-22 source was used to excite the samples. The light yield was measured at a constant temperature of 18°C controlled to better than 1°C. Figure A.6 shows the measured light yield for a subset of about 100 crystals produced by SICCAS in 2017. As observed for transmittance, the crystals show large variation from crystal-to-crystal, which seems in part correlated with chemical composition. Mechanical flaws are also of importance for light yield, i.e. bubbles in the bulk (as discussed in previous paragraphs) increase the light yield, but also introduce non-uniformities, which are not acceptable for resolution requirements. For this set of tested SICCAS crystals, 45% fail NPS level 2 requirements on the light yield. CRYTUR crystals from different crystallizations were investigated as well. Higher crystallization is expected to have lower radiation hardness and potentially also an impact on light yield. The results show that light yield of higher crystallizations is not acceptable for NPS requirements. Discussions with the company for alternate production methods are ongoing

Calibration of inter-laboratory comparison are being explored. Figure A.6 shows a comparison of light yield measurements of the same crystals at CUA and Giessen U. and Caltech, respectively. The results are consistent within the uncertainty. Calibrations with the setup at IPN-Orsay are currently ongoing. A comprehensive report on inter-laboratory calibration will be presented in our next report.

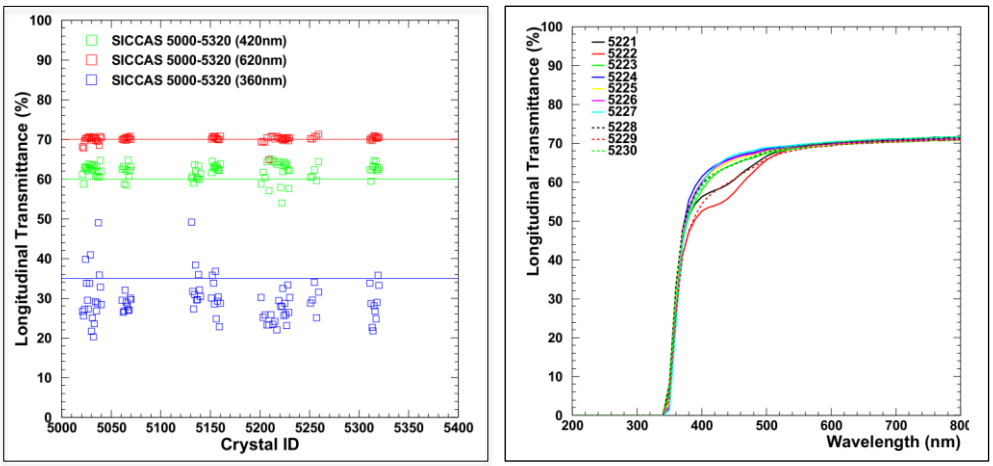

Figure A.5: Optical transmittance for a subset of about 100 crystals produced by SICCAS in 2017. Relatively large variations in transmittance can be observed at 420nm and 360nm, which seem to be correlated with chemical composition. In this set, 14% of the crystals fail specification at 420 nm and 90% the specification at 360 nm (~20% fail with a more relaxed requirement of 25% transmittance at 360nm).

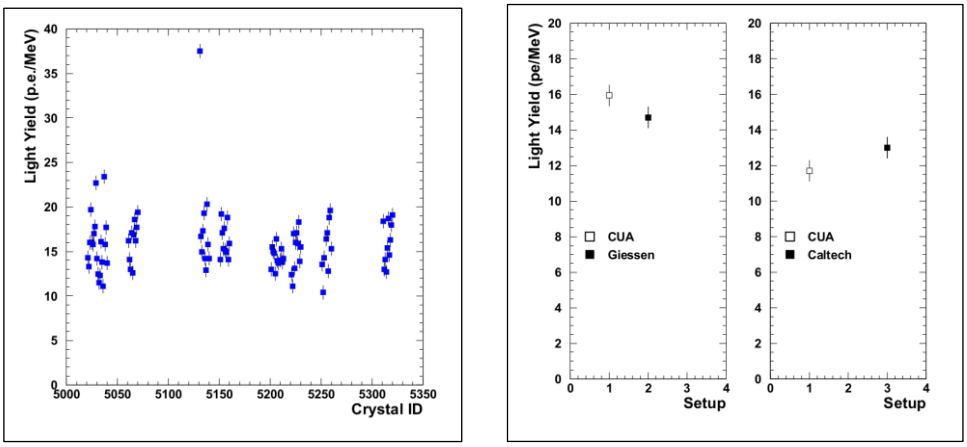

Figure A.6: (left) Light yield for a subset of about 100 crystals produced by SICCAS in 2017. The crystal-to-crystals variations are large and seem to depend on chemical composition, as well as mechanical flaws. (right) Comparison of the light yield measured for the same crystal at CUA (setup=1), and Giessen U. (setup=2) and Caltech (setup=3) respectively. Here, "setup" refers to the facility where the measurements were performed. Details of each setup have been described in our earlier reports. The results from each facility are consistent within statistical and systematic uncertainties.

Development of a SiPM readout for PWO Crystals

We have continued our development of a readout system based on SiPMs for PWO crystals by increasing the coverage of the readout end of the crystal with photosensors. Our previous configuration used a 2x2 array of 3x3 mm^2 SiPMs as shown in Fig. A.7, similar to what is used in the sPHENIX W/SciFi calorimeter. We've now designed and fabricated a new readout board that contains a 3x3 array of 3x3 mm^2 SiPMs (Hamamatsu S13360-025P with 25 μm pixels) as shown in the photo on the right in Fig. A.7. This increases the photosensor coverage by a factor of 9/4 = 2.25. All nine SiPMs are passively summed together so that they can be read out with a single readout channel. Figure A.8 shows a 2x2 SiPM readout board mounted directly on one end of a PWO crystal.

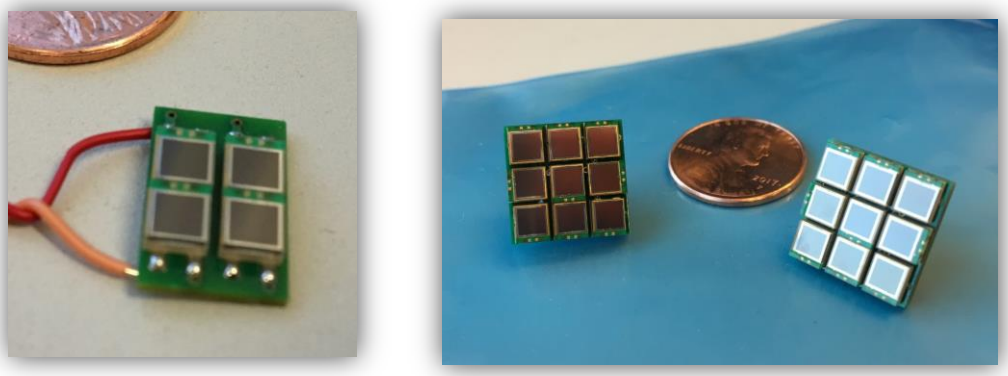

Figure A.7: (left) SiPM readout board containing 2x2 array of 3x3 mm^2 SiPMs. (right) SiPM readout board containing 3x3 array of 3x3 mm^2.

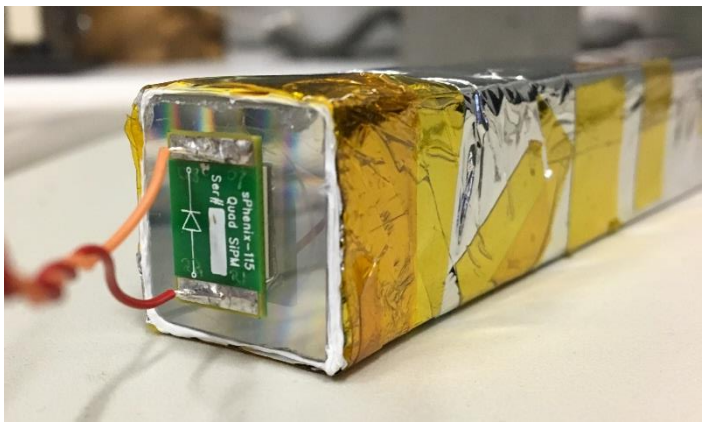

Figure A.8: A 2x2 SiPM readout board mounted directly on one end of a PWO crystal.

Figure A.9 shows the spectra using a ^{137}Cs source for a PWO crystal read out with the 4 SiPMs compared to the 9 SiPMs. After calibrating the spectra to the number of micropixels fired in each case, the relative factor for the increase in light output was ~

2, which is approximately what would be expected in terms of the increased photosensor area coverage. We are now studying the uniformity of light collection in the two cases, and will also measure the relative response using a light guide. However, this will require making a new light guide to match the readout end of the crystal to the two SiPM arrays.

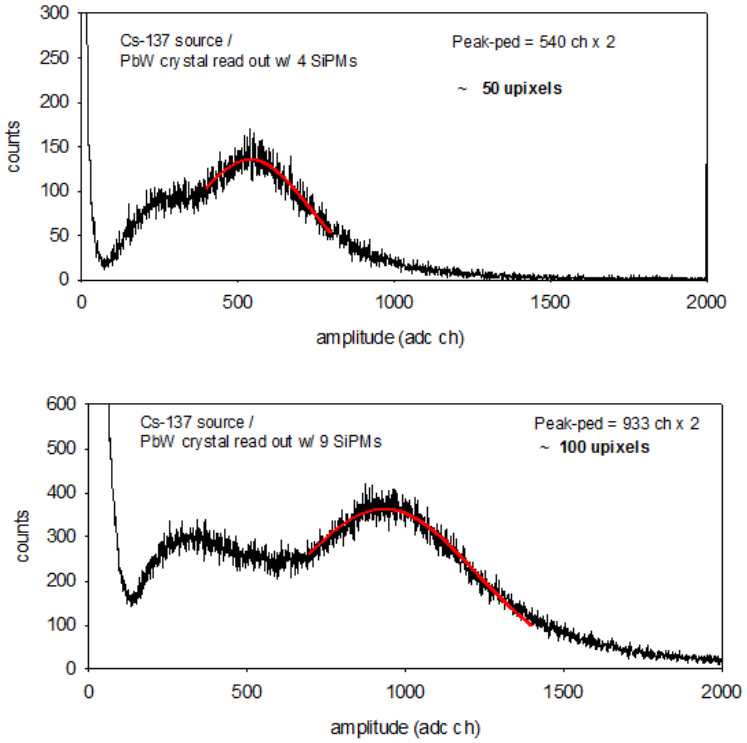

Figure A.9: ^{137}Cs spectra for a PWO crystal read out with a 2x2 array of 3x3 mm^2 SiPMs (top) and 3x3 array of 3x3 mm^{2}of SiPMs. The relative light yield, measured in terms of micropixels fired, is 100/50.

We have also measured the light output of the crystal using the two SiPM arrays using cosmic rays. An example of one of these spectra is shown in Fig. A.10, where the readout from the two ends of the crystal are summed together.

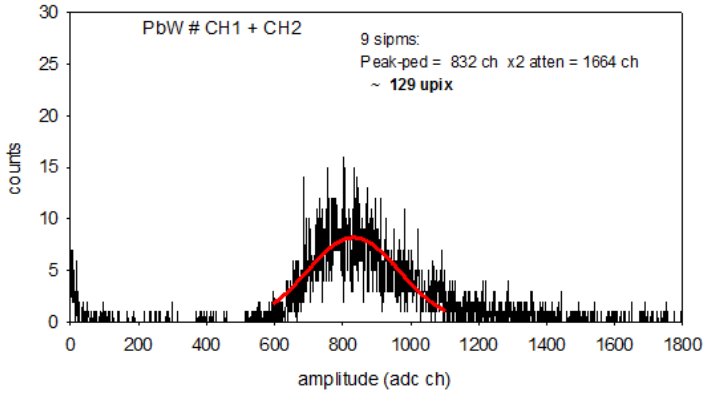

Figure A.10: Cosmic ray spectrum for a PWO crystal read out on each end with a 3x3 mm^2 array of SiPMs.

We plan to continue our tests in the lab in order to compare the relative light output, uniformity and response of the crystal with various types of SiPM readout. We have acquired some of the new Hamamatsu 3x3 mm^2 SiPMs (S13360-025PE) which have reduced noise and crosstalk compared to Hamamatsu's earlier devices (e.g., S12572-025P used in sPHENIX). In addition, we have acquired several new 6x6 mm^2 SiPMs from Hamamatsu (S13360-6025PE), which also have lower noise and reduced cross talk, that will allow us to increase the photosensor coverage of the crystal even further with fewer devices. We plan to continue the tests in the lab with these devices, and also hope to test some of them in the test beam at Fermilab in early 2018.